Research Article | Vol. 28, No. 19 / 14 September 2020 / Optics Express 28072
Optics EXPRESS

Aerosol scattering of vortex beams transmission in hazy atmosphere

CHENGE SHI,[1] LIXIN GUO,[1,3] MINGJIAN CHENG,[1,4] MARTIN PJ LAVERY,[2] AND SONGHUA LIU[1]

[1]School of Physics and Optoelectronic Engineering, Xidian University, Xi'an, Shaanxi, 710071, China
[2]School of Engineering, University of Glasgow, Glasgow G12 8LT, UK
[3]lxguo@xidian.edu.cn
[4]mjcheng@xidian.edu.cn

Abstract: Mie theory is widely used for the simulation and characterization of optical interaction with scattering media, such atmospheric pollutants. The complex refractive index of particle plays an important role in determining the scattering and absorption of light. Complex optical fields, such as vortex beams, will interact with scattering particulates differently to plane wave or Gaussian optical fields. By considering the three typical aerosol particles compositions that lead to haze in the atmosphere, distinctive scattering dynamic were identified for vortex beams as compared to Gaussian beams. Using parameters similar to real world atmospheric conditions, a new aerosol particle model is proposed to efficiently and concisely describe the aerosol scattering. Numerical simulations indicate unique signatures in the scattering dynamics of the vortex beams that can indicate particles composition and also suggest that potentially there is higher optical transmission of vortex beams propagating in certain hazy environments.

1. Introduction

Aerosol pollution has influenced the atmospheric environment, e.g., alterations of the local weather (and climate) [1–3] and the deterioration of visibility and air quality [4]. Therefore, scientific communities have paid attention to the remote sensing of atmospheric aerosol in the last few decades [5,6]. The atmospheric aerosol is a complex multi-particle system that varies with different environments [7]. Under the conditions that the spacing between particles is greater than three times of the particles' diameters or the ratio of particle edge spacing to the wavelength is greater than 0.5 [8], the scattering of aerosol particles are generally approximately independent of each other, and consequently, the single-scattering approximation can be adopted in aerosol scattering modeling. Since 1870, Mie's theory has been proposed to solve the scattering problem of aerosol particle with an assumption that aerosol particles are homogeneous spherical. Various analytical solutions of the Mie scattering model of spherical particles under plane wave incidence by Lorenz [9] and Mie [10], the scattering law of uniform spherical particles with arbitrary diameter and composition was examined. Since then, they have established a Lorenz-Mie theory that provides a theoretical basis for complex particle scattering problems. However, the water vapor in the atmosphere may affect the relative humidity and size of aerosol particles, resulting in determining the scattering and absorption feature. Mie theory has been extended to a concentric sphere model, and the scattering and absorption coefficients of aerosol particles with water-soluble coatings and insoluble nuclear were calculated [11]. Based on the generalized Lorenz-Mie theory (GLMT) [12], the scattering problem of elliptical beams can be solved [13–14], and the scattering models of spherical coated and multilayered particles located in an arbitrary beam have been developed [15–16]. When it comes to the light scattering of non-spherical aerosol particles (arbitrary shapes or aggregation particles), several numerical computation methods have been adopted, such as Finite-difference time domain (FDTD) method [17], Discrete Dipole Approximation, Ray Tracing [18], physical-geometric optics hybrid method [19], and so on.

#401293 https://doi.org/10.1364/OE.401293
Journal © 2020 Received 1 Jul 2020; revised 19 Aug 2020; accepted 24 Aug 2020; published 9 Sep 2020

Optics EXPRESS

Traditionally scattering theory has focused on optical beams with a Gaussian amplitude profile. Consequently, Gaussian laser sources are widely used to study the scattering and attenuation characteristics of aerosol particles. In 2011, Mackowski and Mishchenko used the T-matrix method to study the mechanism of Gaussian beam propagating in random discrete particle systems [20]. A numerical method was introduced by Han in 2012 to describe the scattering characteristics of arbitrarily shaped particles with multiple inclusions illuminated by Gaussian beam [21], which provides useful insights for the study of composite particles. In 2013, the radiation force and torque exerted on a chiral sphere by polarized Gaussian beams were studied with GLMT [22].

For vortex beams that carry orbital angular momentum (OAM), have helically phased wavefronts [23] that will interact with scattering structures in a unique manner. Vortex beams have been widely considered for use in a broad range of applications including spatial multiplexing for high capacity communications [24–25] and radar application [26]. Therefore, studying the interaction mechanism between vortex beams and different materials is of theoretical guiding significance for analyzing the transmission capacity of vortex beams in various scattering medium. Mitri [27] investigated the arbitrary scattering of an unpolarized high-order Bessel vortex beam by a homogeneous water sphere in air. Scattering of two interaction homogeneous uniaxial anisotropic spheres illuminated by a Laguerre-Gaussian (LG) vortex beam was studied with GLMT [28], and described the internal and near-surface field of a NaCl crystal, which is useful for the further research on the propagation of arbitrary vortex beam in scattering medium with periodic structure. In 2016, an experiment on the transmittance of LG beams and Gaussian beams in polystyrene aqueous solution has been done [29], a higher transmittance of LG beams was observed in the diffusive region compared with the Gaussian beam, and the LG beams with higher value of topological charge l showed a higher received signal than those with lower l values. Yang [30] and Chen [31] investigated the scattering of arbitrary shaped particles illuminated by high-order Bessel vortex beams using the FDTD algorithm and the multilevel fast multilevel fast multipole algorithm, respectively. The results would provide new efficient methods to study the interactions between nondiffracting vortex beams and complex particles. The interaction mechanism between particles and vortex beams has hardly been applied to aerosol environments, Huang [32] investigated the scattering and polarization characteristics of marine atmospheric aerosol illuminated by HG incident beams using an equivalent humidity model. The study concluded that the HG beam was more sensitive to the change in relative humidity than other beams (i.e., plane wave and Gaussian beam), consequently offering advantages in remote sensing of aerosol. While, the humidity equivalent model is not suitable for all types of aerosol particles, especially for non-deliquescent aerosol particles, the double-layer concentric sphere model provides a more reasonable and accurate approach to examine the effect of relative humidity on scattering characteristics of the non-deliquescent aerosol particles. However, the double-layer concentric sphere model also has difficulty in dealing with the soluble particles. Therefore, it is necessary to develop a new model that overcomes limitations from the humidity equivalent model and the double-layer concentric sphere model for more efficiently and accurately, modeling the scattering of atmospheric aerosol particles.

Based on the GLMT, this paper focuses on simulating the scattering, absorption and extinction efficiency factors of aerosol particles illuminated by Gaussian vortex beams. Results show that the scattering and absorption of high-order Gaussian vortex beams by particles is smaller than those of traditional Gaussian beam, which means Gaussian vortex beams propagating in certain haze aerosol medium have the higher optical transmission when only considering the single scattering. In addition, when a spherical model is adopted to simulate the atmospheric aerosols, there is a lack of an approximate model that can more realistically describe the intermediate state of deliquescence. A geometric relationship is proposed to modified the description model of

Optics EXPRESS

aerosol and proved that can achieve the purpose of better describing the physical characteristic of deliquescence in a neutral manner.

2. The theoretical model

2.1. Scattering model of a vortex beam

In a cylindrical coordinate system, the electric field of a Gaussian vortex beam at the source plane is expressed as:

$$E(r,\varphi) = E_0\left(\frac{r}{w_0}\right)^l \exp\left(-\frac{r^2}{{w_0}^2}\right)\exp(il\varphi) \tag{1}$$

where l represents the OAM mode (topological charge) of vortex beam, w_0 is the beam width, E_0 is the normalized amplitude, and (r, φ) is the two-dimensional position vector.

Based on the vector spatial angular spectrum theory [33], the radial components of the spatial electric field and magnetic field can be obtained from the stationary phase and the integral local approximation methods [34]:

$$\begin{aligned} E_r = {} & \frac{(-i)^{l-1}k{w_0}^{l+2}z}{2^l(r^2+z^2)^{l/2+1}}\left(n+\frac{1}{2}\right)^l E_0 \times \exp\left[-\frac{{w_0}^2}{4(r^2+z^2)}\left(n+\frac{1}{2}\right)^2\right] \\ & \times \exp\left(ik\sqrt{r^2+z^2}\right)\cos\varphi\exp(-il\varphi) \end{aligned} \tag{2}$$

$$\begin{aligned} H_r = {} & \left(\frac{2}{k}\left(n+\frac{1}{2}\right)^2\cos^2\varphi - kz^2\right)\frac{(-i)^{l+1}{w_0}^{l+2}(n+1/2)^l}{2^l(r^2+z^2)^{(l+3)/2}} \times H_0\exp\left[-\frac{{w_0}^2}{4(r^2+z^2)}\left(n+\frac{1}{2}\right)^2\right] \\ & \times \exp\left(ik\sqrt{r^2+z^2}\right)\sin\varphi\exp(-il\varphi) \end{aligned} \tag{3}$$

In a cylindrical coordinate system, beam shape coefficients (BSCs) can be obtained from the following relationships:

$$g^m_{n,TM} = \frac{Z^m_n}{2\pi E_0}\int_0^{2\pi} E_r(r,\theta,\phi)\exp(-im\phi)d\phi \tag{4}$$

$$g^m_{n,TE} = \frac{Z^m_n}{2\pi H_0}\int_0^{2\pi} H_r(r,\theta,\phi)\exp(-im\phi)d\phi \tag{5}$$

Substituting Eqs. (2–3) into Eqs. (4–5), the BSCs of Gaussian vortex beams are derived as:

$$g^m_{n,TM} = \begin{cases} \frac{-(-i)^{l+1}Z^m_n{w_0}^{l+2}(n+0.5)^l kz}{2^{l+1}(r^2+z^2)^{l/2+1}}e^{-\frac{{w_0}^2}{4}\frac{(n+0.5)^2}{(r^2+z^2)}}e^{ik\sqrt{r^2+z^2}} & m = -l\pm 1 \\ 0 & \text{the others} \end{cases} \tag{6}$$

$$g^m_{n,TE} = \begin{cases} \pm\left(\frac{(n+0.5)^2}{2k} - kz^2\right)\frac{(-i)^{l+2}Z^m_n{w_0}^{l+2}(n+0.5)^l}{2^{l+1}(r^2+z^2)^{(l+3)/2}}e^{ik\sqrt{r^2+z^2}}e^{-\frac{{w_0}^2}{4}\frac{(n+0.5)^2}{(r^2+z^2)}} & m = \pm 1 - l \\ \pm\frac{(-i)^{l+1}Z^m_n{w_0}^{l+2}(n+0.5)^{l+2}}{2^{l+2}(r^2+z^2)^{(l+3)/2}}e^{ik\sqrt{r^2+z^2}}e^{-\frac{{w_0}^2}{4}\frac{(n+0.5)^2}{(r^2+z^2)}} & m = \pm 3 - l \\ 0 & \text{the others} \end{cases} \tag{7}$$

with

$$Z^m_n = \begin{cases} \frac{2n(n+1)i}{2n+1} & m = 0 \\ \frac{(-2i/2n+1)^{|m|-1}}{2n+1} & m \neq 0 \end{cases} \tag{8}$$

Optics EXPRESS

The above BSCs of Gaussian vortex beams can be applicable to all types of scattering targets because the BSCs are only influenced by beam shapes.

Once the scattering coefficients and BSCs are determined, according to the GLMT, the scattering efficiency factor (Qsca), extinction efficiency factor (Qext), and absorption efficiency factor (Qabs) in hazy atmosphere can also be calculated as follows [35]:

$$Q_{sca} = \frac{4}{k^2a^2}\sum_{n=1}^{\infty}\sum_{m=-n}^{n}\frac{2n+1}{n(n+1)}\frac{(n+|m|)!}{(n-|m|)!}(|a_n|^2|g_{n,TM}^m|^2 + |b_n|^2|g_{n,TE}^m|^2) \tag{9}$$

$$Q_{ext} = \frac{4}{k^2a^2}\mathrm{Re}[\sum_{n=1}^{\infty}\sum_{m=-n}^{n}\frac{2n+1}{n(n+1)}\frac{(n+|m|)!}{(n-|m|)!}(a_n|g_{n,TM}^m|^2 + b_n|g_{n,TE}^m|^2)] \tag{10}$$

$$Q_{abs} = Q_{ext} - Q_{sca} \tag{11}$$

where a_n and b_n are the scattering coefficients of plane wave suggested by Mie. We adopt the corresponding mathematical expressions on the variable scattering models to distinguish different boundary conditions. The expansion coefficients of scattered field are expressed as:

$$\begin{cases} A_{mn} = a_n g_{n,TM}^m \\ B_{mn} = b_n g_{n,TE}^m \end{cases} \tag{12}$$

Considering the far-field approximation, the electric field components of the scattered field at a long distance are given as:

$$\begin{cases} E_r = 0 \\ E_\theta = iE_0S_2\exp(ikr)/(kr) \\ E_\varphi = -E_0S_1\exp(ikr)/(kr) \end{cases} \tag{13}$$

where S_1 and S_2 are scattering amplitude functions [15]:

$$\begin{cases} S_1 = \sum\limits_{n=1}^{\infty}\sum\limits_{m=-n}^{n}\frac{2n+1}{n(n+1)}[ma_n g_{n,TM}^m \pi_{|m|n}(\cos\theta) + ib_n g_{n,TE}^m \tau_{|m|n}(\cos\theta)]\exp(im\varphi) \\ S_2 = \sum\limits_{n=1}^{\infty}\sum\limits_{m=-n}^{n}\frac{2n+1}{n(n+1)}[imb_n g_{n,TE}^m \pi_{|m|n}(\cos\theta) + a_n g_{n,TM}^m \tau_{|m|n}(\cos\theta)]\exp(im\varphi) \end{cases} \tag{14}$$

with

$$\begin{cases} \pi_{mn}(\cos\theta) = \frac{P_n^m(\cos\theta)}{\sin\theta} \\ \tau_{mn}(\cos\theta) = \frac{d}{d\theta}P_n^m(\cos\theta) \end{cases} \tag{15}$$

where $P_n^m(\cos\theta)$ represents the first-class associated Legendre polynomials that have order m and degree n. Therefore, the differential scattering cross sections (DSCS) of far-field scattering is defined as:

$$DSCS = (|S_1|^2 + |S_2|^2)\lambda^2/\pi \tag{16}$$

2.2. Different models of aerosol particle

(1) Humidity equivalent spherical particle model

Due to the inherent variation's atmospheric conditions, any aerosol particulate investigation must consider the effect of water. A humidity equivalent model proposes that the aerosol particle are solid particles that are uniformly covered in water vapor. Therefore, we can get the complex refractive index of the humidity equivalent particle from those of solid particles and water. The

Optics EXPRESS

size of equivalent aerosol particles at a certain relative humidity can be expressed by the Hanel's model [36] as follows:

$$R_{wet} = R_0(1 - H_r)^{-(1/C)} \tag{17}$$

where R_0 is the size of solid aerosol, Hr is the relative humidity, and C is a constant coefficient that reflects the aerosol environment. In this study, the value of the polluted atmosphere, C=4.4, was employed. After obtaining the size of humidity equivalent particle, the complex refractive index can be calculated by:

$$\begin{aligned} m_r &= m_{rw} + (m_{r0} - m_{rw})(R_0/R_{wet})^3 \\ \frac{m_i}{{m_r}^2+2} &= \frac{m_{iw}}{{m_{rw}}^2+2} + \left(\frac{m_{i0}}{{m_{r0}}^2+2} - \frac{m_{iw}}{{m_{rw}}^2+2}\right)\left(\frac{R_0}{R_{wet}}\right)^3 \end{aligned} \tag{18}$$

where $m_0 = m_{r0} - im_{i0}$ and $m_w = m_{rw} - im_{iw}$ are the complex refractive indices of solid aerosol particles and water, respectively. The humidity equivalent model assumes that the aerosol particles are single homogeneous spheres with various complex refractive indices and physical size. The Mie scattering coefficients, a_n and b_n, are consistent with the expansion coefficients of the spherical vector wave function, as:

$$\begin{cases} a_n = \frac{\mu m^2 j_n(mx_h)[x_h j_n(x_h)]' - \mu_1 j_n(x_h)[mx_h j_n(mx_h)]'}{\mu m^2 j_n(mx_h)[x_h h_n^{(1)}(x_h)]' - \mu_1 h_n^{(1)}(x_h)[mx_h j_n(mx_h)]'} \\ b_n = \frac{\mu_1 j_n(mx_h)[x_j j_n(x_h)]' - \mu j_n(x_h)[mx_h j_n(mx_h)]'}{\mu_1 j_n(mx_h)[x_h h_n^{(1)}(x_h)] - \mu h_n^{(1)}(x_h)[mx_h j_n(mx_h)]'} \end{cases} \tag{19}$$

where the size parameter (x_h) is $2\pi R_{wet}/\lambda$ and λ is the wavelength, μ and μ_1 are the permeability of background medium and aerosol particle, respectively. The functions $j_n(x)$ and $h_n^{(1)}(x)$ represent the spherical Bessel and Hankel functions of the first kind, respectively.

(2) Double -layer concentric sphere particle model

Some particles in the atmosphere can also be regarded as nucleated particles, i.e. solid particles covered by a layer of water vapor. A double-sphere concentric model outperforms a single sphere model with regard to simulating the scattering characteristics of non-deliquescent aerosol particles. As the spherical vector wave function of the inner field is dependent on two different regions (media), new mathematical expressions of the Mie scattering coefficients (a_n and b_n) can be obtained from the continuity of the tangential components of electric and magnetic fields at the surface and interface:

$$\begin{cases} a_n = \frac{H_n^A \psi_n(ka) - m\psi'_n(ka)}{H_n^A \xi_n^{(1)}(ka) - m\xi_n'^{(1)}(ka)} \\ b_n = \frac{mH_n^B \psi_n(ka) - \psi'_n(ka)}{mH_n^B \xi_n^{(1)}(ka) - \xi_n'^{(1)}(ka)} \end{cases} \tag{20}$$

and

$$\begin{cases} H_n^A = \frac{Q_n^d \xi_n'^{(1)}(k_1 a) + \xi_n'^{(2)}(k_1 a)}{Q_n^d \xi_n^{(1)}(k_1 a) + \xi_n^{(2)}(k_1 a)} \\ H_n^B = \frac{Q_n^c \xi_n'^{(1)}(k_1 a) + \xi_n'^{(2)}(k_1 a)}{Q_n^c \xi_n^{(1)}(k_1 a) + \xi_n^{(2)}(k_1 a)} \end{cases} \tag{21}$$

$$\begin{cases} Q_n^d = \frac{k_1 \zeta_n(k_1 b)\psi'_n(k_2 b) - k_2 \zeta'_n(k_1 b)\psi_n(k_2 b)}{k_2 \xi'_n(k_1 b)\psi_n(k_2 b) - k_1 \xi_n(k_1 b)\psi'_n(k_2 b)} \\ Q_n^c = \frac{k_1 \zeta'_n(k_1 b)\psi_n(k_2 b) - k_2 \zeta_n(k_1 b)\psi'_n(k_2 b)}{k_2 \xi_n(k_1 b)\psi'_n(k_2 b) - k_1 \xi'_n(k_1 b)\psi_n(k_2 b)} \end{cases} \tag{22}$$

where $\psi_n(x) = xj_n(x)$ and $\zeta_n(x) = xh_n^{(1)}(x)$ are Ricatti-Bessel functions. k and k_1 are wave numbers propagating in background medium and aerosol particles, respectively.

(3) Modified humidity equivalent model

Optics EXPRESS

In the humidity equivalent model outlined above, the value of the constant coefficient C only depends on the types of aerosol, while the influence of relative humidity is ignored. For instance, the constant coefficient C equals to 3.9 for the marine atmosphere, whereas 4.4 for the polluted atmosphere. In other word, the constant coefficient C is highly affected by the atmospheric environment, indicating that it should reflect the hygroscopicity of various aerosol particles or the humidity. Therefore, the constant coefficient C in the humidity equivalent model needs to be modified for solid particles covered by water vapor. The mass ratios of the water vapor to the dry aerosol particle and the relative humidity satisfy the following relation [37]:

$$\frac{m_w}{m_0} = \bar{\mu}\frac{Hr}{1 - Hr} \tag{23}$$

where m_w and m_0 represent the mass of water vapor and dry particles respectively, $\bar{\mu}$ denoting a linear augmenting factor of mass as a constant. The relative humidity in a double-layer concentric sphere model can be expressed by:

$$Hr = \frac{\rho_w(a^3 - b^3)}{\bar{\mu}\rho_0 b^3 + \rho_w(a^3 - b^3)} \tag{24}$$

where ρ_w and ρ_0 are the density of water vapor and dry particles, respectively.

When scattering described by the double-layer concentric sphere model is covered by a layer of water vapor, we can consider this as a humidity equivalent model, where the outer radius a and inner radius b can represent the wet particle's radius (R_{wet}) and dry particle's radius (R_0) of the humidity equivalent model. Using a simple geometric relationship, the core-containing double-layer concentric sphere model and the humidity equivalent model can be combined by substituting the relative humidity, the internal and external dimensions of the double-layer sphere into Eq. (17), resulting in obtaining the constant C of the modified humidity equivalent model with the expression as follows:

$$C = -1/\log_{(1-Hr)}{}^{(a/b)} \tag{25}$$

Figure 1 demonstrates the relative humidity and correction constants of carbonaceous aerosol particles in the modified humidity equivalent model as a function of the inner and outer diameter size ratios in the concentric double-layer spherical model. From Fig. 1(a), it is found that the relative humidity of the particles decreases along with an increase in the ratio of inner diameter to outer diameter of particles, indicating that the inner and outer diameter size ratio is larger in the concentric double-layer spherical model (the thinner outer coating layer and the smaller moisture content) while the relative humidity in the modified humidity equivalent model will be lower. At the same time, the relative humidity of particles is preserved at a relatively high level with a small change when the inner and outer diameter size ratio is small. As the ratio becomes larger, on the contrary, the decline rate of the relative humidity increases rapidly by the fact that water vapor gradually become less dominant. The corresponding correction constant -1/C in the modified humidity equivalent model can be obtained from the relative humidity. It is also shown that the correction constant has a prominent approximate linear relationship with the inner and outer diameter size ratio.

2.3. Complex refractive index of particles in hazy atmosphere

Haze pollution is the main phenomenon that mainly reduces the visibility due to the scattering and absorption effects of aerosol particles in the hazy atmosphere. Water-soluble substances (e.g., ammonium sulfate, sulfuric acid, ammonium nitrate, etc.) and carbon constituent particles (elemental carbon and organic carbon) are the main chemical substances that cause the reduction of atmospheric visibility in the haze pollution [38]. The complex refractive indices of these particle components are given in Table 1. In addition, the complex refractive index of water (m_w)

Optics EXPRESS

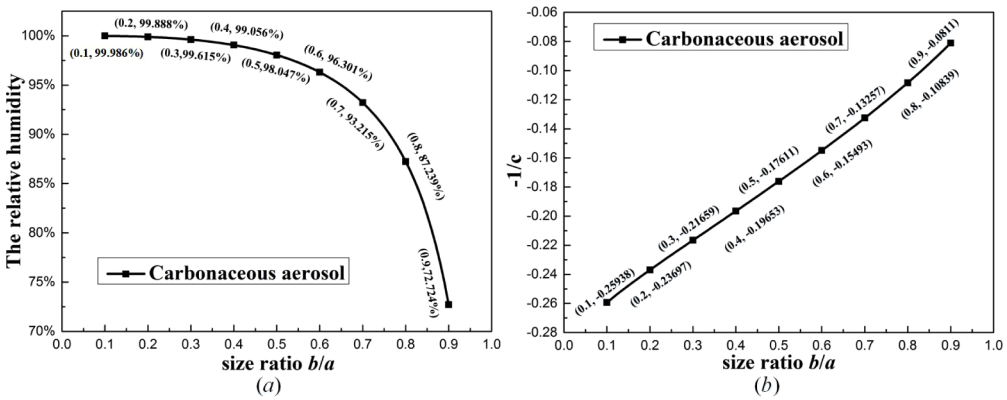

Fig. 1. The relative humidity (a) and correction constants (b) with different ratios of inner and outer diameter Schemes follow the same formatting.

is 1.333-1.96×$10^{-9}i$. As the composition and content of aerosol particles in hazy atmosphere are dependent on regions and times, a continuous monitoring system is required to provide a long-term observation and statistic. Previous studies suggested that the main components that cause the haze in winter were Carbonaceous aerosol, Ammonium sulfate and Ammonium nitrate, their proportions were 47%, 28% and 25%, which were employed in the following simulations.

Table 1. The names, proportions and complex refractive indices of main particles causing scattering and absorption in hazy atmosphere

Name	Ammonium sulfate	Ammonium nitrate	Carbonaceous aerosol
Complex refractive index	1.520-1.0*$10^{-7}i$	1.554-1.0*$10^{-8}i$	1.750-i*0.44
Proportion	28%	25%	47%

3. Discussions and analyses

In this section, the numerical results of the scattering, absorption and extinction efficiency factors of aerosol particles illuminated by Gaussian vortex beams in hazy atmosphere are discussed in detail. The schematic diagram of aerosol remote sensing in hazy atmosphere based on the scattering of vortex beams and two typical modeling methods of aerosol particles is displayed in Fig. 2. The numerical results are simulated by the modified humidity equivalent model. Furthermore, a typical humidity equivalent model and a concentric double sphere model are adopted to validate the modified humidity equivalent model. Based on the analytical equations in the previous section, the parameters of the humidity equivalent model and double-layer concentric sphere model are set as Table 2. The following parameters are assumed unless otherwise specified: the topological charge of incident vortex beam is set to l=1, the wavelength (λ) and beam width (w_0) are 0.55 μm and 1.0 μm, respectively. The inner radius of the particle for the concentric double layer sphere model is equal to that of dry particles for the equivalent humidity model.

Table 2. Parameters of particles in different model

models	Double-layer sphere	Humidity equivalent model
parameters	b=0.8a	Hr=0.8
	b=0.5μm	R_0=0.5μm

Optics EXPRESS

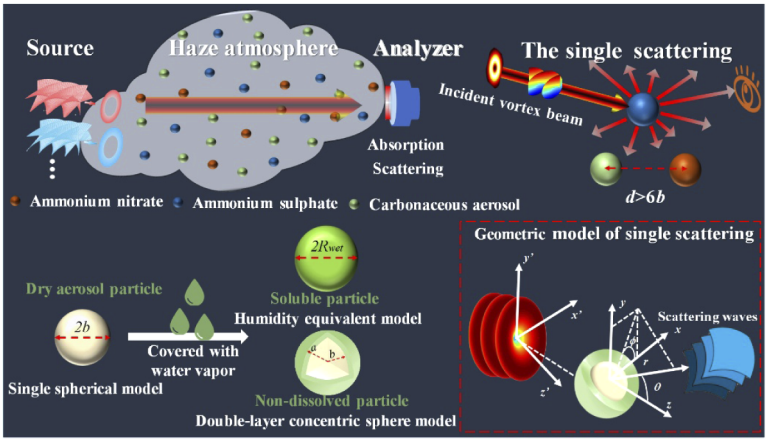

Fig. 2. Schematic diagram of aerosol remote sensing in hazy atmosphere based on the scattering of vortex beams.

Figure 3 shows the comparison results of the double-layer concentric model (b=0.8a) for extinction (a), scattering (b) and absorption (c) efficiency factors of three typical aerosol particles (ammonium sulfate, ammonium nitrate and carbonaceous aerosol particles) in the hazy atmosphere. The complex refractive indices of ammonium sulfate, ammonium nitrate and carbonaceous aerosol particles are 1.520-10^{-7}i, 1.554-10^{-8}i and 1.750-0.44i, respectively. For ammonium sulfate and ammonium nitrate particles (black and red lines), the scattering and absorption efficiency factors show a similar tendency in magnitude and oscillation degrees while different change trends for the carbonaceous aerosol particles (blue line) mainly due to a larger difference in the complex refractive indices. The complex refractive index of particle plays an important role in determining the scattering and absorption of light. The real and imaginary parts of the complex refractive index can highly influence the scattering and absorption. The real part of the complex refractive index for carbonaceous aerosol particles has the same order of magnitude as that of ammonium salt particles with a large value, in addition, the imaginary part of the complex refractive index of carbonaceous aerosol particles has several orders of magnitude higher than those of the other two types of particles, which can be referred to Table 1. Consequently, the absorption efficiency factors of ammonium sulfate and ammonium nitrate particles are much smaller (approaching 0) than that of carbonaceous aerosol particles, but the scattering efficiency factors are larger. As extinction is equal to the sum of absorption and scattering, so the extinction efficiency factors of carbonaceous aerosol particles, ammonium sulfate and ammonium nitrate particles are close to each other. Given the differences between the complex refractive index and calculation results for different particles, it can be concluded that the imaginary part of the complex refractive index may affect the oscillation degree of the result curves of the efficiency factors to some extent. Atmospheric aerosol remote sensing detection usually requires both the scattering and the absorption characteristics for an aerosol particle composition analysis.

Figure 4 shows the efficiency factors for Gaussian vortex beams that transmit with different topological charges (l=0 (a), 1 (b) and 2 (c)) in the hazy atmosphere, where the joint effects of Carbonaceous aerosol particles, Ammonium sulfate particles, and Ammonium nitrate particles are superimposed with their own weight (their weights are shown in Table 1). The double-layer concentric model (b=0.8a) is chosen here, the wavelength (λ) and waist radius (w_0) of incident beams are 0.55μm and 1.0μm, respectively. Given that the topological charge number is 0, the vortex beam evolves into a traditional Gaussian beam. It is clearly seen that the efficiency factors

Optics EXPRESS

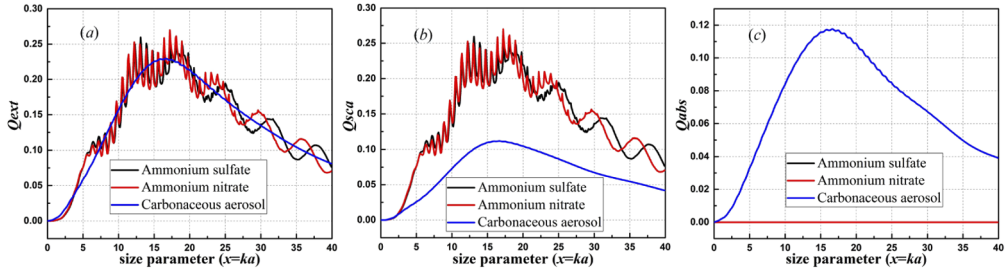

Fig. 3. The comparison of efficiency factors (extinction (a), scattering (b) and absorption (c)) for three typical aerosol particles in hazy atmosphere.

for Gaussian vortex beams carrying a high-order topological charge number are smaller than those for Gaussian beams, the reason is that the beam is incident on axis and the intensity null at the center of the OAM beams. Therefore, considering the scattering of each particle as a single scattering when transmitting in the same aerosol environment, the penetration ability of Gaussian vortex beam would be better than Gaussian beam.

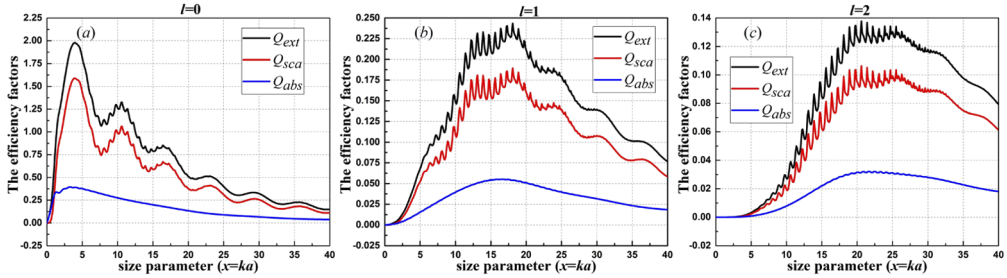

Fig. 4. Weighted average of extinction, scattering and absorption efficiency factors of Gaussian vortex beams carrying different topological charges (l=0 (a), l=1 (b) and l=2 (c)) in hazy atmosphere.

Figure 5 displays the weighted efficiency factors of aerosols in hazy atmosphere illuminated by Gaussian vortex beam with beam width w_0=0.5 μm (a), 1.0 μm (b) and 1.5 μm (c). It is clearly that the scattering and absorption efficiency factors increase with the increase of beam-waist radius. In general, the increasing of beam width will continuously enhance the scattering and absorption effects, since the beam with a larger beam width can let more energy illuminate on particles. Therefore, the Gaussian vortex beam with a small beam width will has a stronger penetration. In addition, the peaks of extinction, scattering and absorption efficiency factors are different with the change of beam width, which is very important for the selection of waveband. The good matching of beam width and wavelength can get a better transmission.

Figure 6 presents the extinction (a), scattering (b) and absorption (c) efficiency factors of Gaussian vortex beams given that the atmospheric humidities in haze are at 70%, 80% and 90%. The results show that the scattering effect enhanced and the absorption effect gradually weaken in hazy atmosphere as the relative humidity increased. While the relative refractive index of pure water (m) was $1.333\text{-}1.96\times10^{-9}i$, both the real and imaginary parts of the relative refractive index for the water vapor are smaller than those for the three aerosol particles in hazy atmosphere, which means that the scattering efficiency factor is larger and the absorption efficiency factor is smaller for water vapor. As the relative humidity is higher, therefore, the results are closer to those of pure water vapor who has a stronger scattering and weaker absorption.

Optics EXPRESS

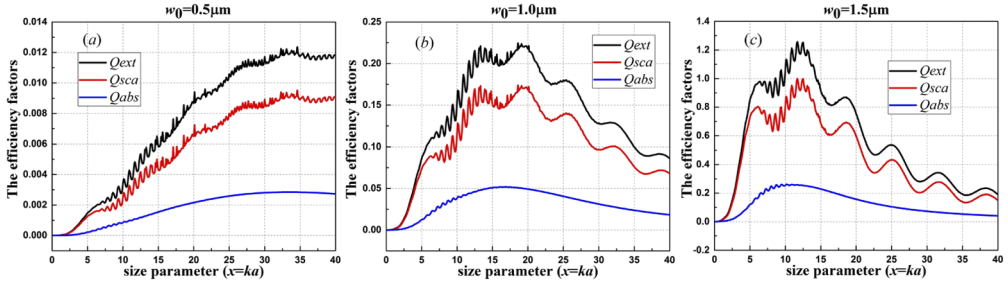

Fig. 5. Weighted average of extinction, scattering and absorption efficiency factors of Gaussian vortex beam with various beam width w_0 (0.5 μm (a), 1.0 μm (b) and 1.5 μm (c)) in hazy atmosphere.

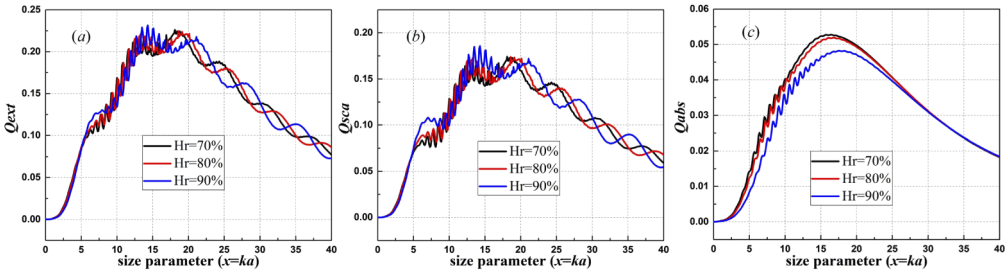

Fig. 6. Weighted average of efficiency factors (extinction (a), scattering (b) and absorption (c)) of Gaussian vortex beams propagating in hazy atmosphere with different relative humidity Hr.

Figures 7 and 8 show the efficiency factors (extinction (7(a)), scattering (7(b)) and absorption (7(c))) and DSCS (E plane (8(a)) and H plane (8(b))) for different particle models in hazy atmosphere. The calculated parameters for those particle models are shown in Table 2. It is prominent that all three efficiency factors decrease with the solubility of aerosol particles in hazy atmosphere. The efficiency factors for the double-layer spherical particle model and the humidity equivalent model provide upper and lower bounds of the results for the modified humidity equivalent model. The double-layer spherical particle model overestimates the efficiency factors in the case that there are a large number of soluble particles in the atmospheric aerosol, whereas the humidity equivalent model underestimates them for the atmospheric aerosol with a lot of non-deliquescent aerosol particles. In contrast, the results of the modified humidity equivalent model are more consistent with the trend of the DSCS results of the double-layer sphere model compared with those of the humidity equivalent model, as its solubility is closer to non-deliquescent particles with the modified parameters shown in Table 2. Overall, the results demonstrate that the modified humidity equivalent model provides more reliable and accurate simulations in atmospheric aerosol remote sensing. Therefore, the modified humidity equivalent model proposed in this study may be more applicable for the calculation of aerosol particles with moderate deliquescence or real aerosol media. Besides, it provides the threshold reference to determine the constant coefficient C for soluble aerosol particles with different deliquesce degrees.

Optics EXPRESS

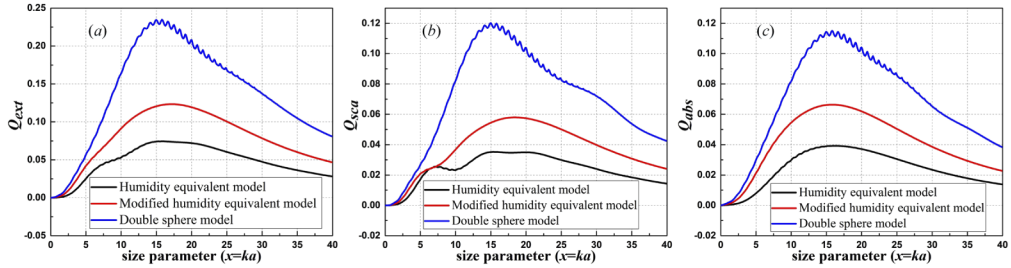

Fig. 7. The comparison of weighted efficiency factors (extinction (a), scattering (b) and absorption (c)) among three different particle models.

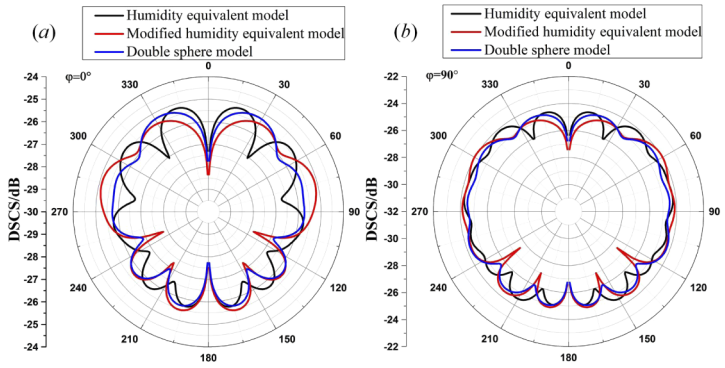

Fig. 8. The comparison of differential scattering cross sections ((a) E plane and (b) H plane) among different particle models for Carbonaceous particles.

4. Conclusion

This study investigated the scattering models of vortex beams in hazy atmosphere for three typical aerosol particles (ammonium sulfate, ammonium nitrate and carbonaceous aerosol particles) and analyzed their absorption and scattering characteristics. Numerical simulations indicate that the complex refractive index of aerosol particles play an important role in determining the scattering and absorption characteristics of vortex beams. This result highlights the possibility that chemical composition of aerosol particles can be derived by measuring the scattering and absorption of vortex beams for remote sensing of the hazy atmosphere. We further note that these simulations show that the attenuation of the Gaussian vortex beams is smaller than that of the traditional Gaussian beam in propagating through aerosol particles. Three types of single-scattering models were adopted to investigate the scattering of Gaussian vortex beams in the haze atmosphere. The humidity equivalent model performs better for modeling soluble aerosol particles, while the double-layer concentric sphere model outperforms in modeling the non- deliquescent particles. We outlined a modified humidity equivalent model to accurately simulate the scattering of a mixed particle system (i.e., atmospheric aerosol), which may be beneficial in environmental remote sensing.

Funding

National Natural Science Foundation of China (61431010, 61627901, 61901336, 61905186); Foundation for Innovative Research Groups of the National Natural Science Foundation of China (61621005); Natural Science Foundation of Shaanxi Province (2020JQ-286).

Optics EXPRESS

Disclosures

The authors declare no conflicts of interest.

References

1. D. Rosenfeld, U. Lohmann, G. B. Raga, C.D. Odowd, M. Kulmala, S. Fuzzi, A. Reissell, and M.O. Andreae, "Flood or Drought: How Do Aerosols Affect Precipitation?" Science **321**(5894), 1309–1313 (2008).
2. M. O. Andreae and D. Rosenfeld, "Aerosol–cloud–precipitation interactions. Part 1. The nature and sources of cloud-active aerosols," Earth-Sci. Rev. **89**(1-2), 13–41 (2008).
3. R. P. Turco, R. C. Whitten, O. B. Toon, J. B. Pollack, and P. Hamill, "OCS, stratospheric aerosols and climate," Nature **283**(5744), 283–285 (1980).
4. A. Molnár, K. Imre, Z. Ferenczi, G. Kiss, and A. Gelencsér, "Aerosol hygroscopicity: Hygroscopic growth proxy based on visibility for low-cost PM monitoring," Atmos. Res. **236**, 104815 (2020).
5. Y. M. Noh, D. Müller, D. H. Shin, H. Lee, J. S. Jung, K. H. Lee, M. Cribb, Z. Q. Li, and Y. J. Kim, "Optical and microphysical properties of severe haze and smoke aerosol measured by integrated remote sensing techniques in Gwangju, Korea," Atmos. Environ. **43**(4), 879–888 (2009).
6. X. Xia, H. Che, J. Zhu, H. Chen, Z. Cong, X. Deng, X. Fan, Y. Fu, P. Goloub, H. Jiang, Q. Liu, B. Mai, P. Wang, Y. Wu, J. Zhang, R. Zhang, and X. Zhang, "Ground-based remote sensing of aerosol climatology in China: Aerosol optical properties, direct radiative effect and its parameterization," Atmos. Environ. **124**(124), 243–251 (2016).
7. C. Pilinis and X. Li, "Particle shape and internal inhomogeneity effects on the optical properties of tropospheric aerosols of relevance to climate forcing," J. Geophys. Res. **103**(D4), 3789–3800 (1998).
8. M. Q. Brewster and C. L. Tien, "Radiative transfer in packed fluidized beds: dependent versus independent scattering," J. Heat Trans-T. Asme. **104**(4), 573–579 (1982).
9. L. Lorenz, "Upon the light reflected and refracted by a transparent sphere," *Vidensk Selsk Shrifter*, 61–62 (1890).
10. G. Mie, "Articles on the optical characteristics of turbid tubes, especially colloidal metal solutions," Ann. Phys-Berlin. **330**(3), 377–445 (1908).
11. C. S. Sloane, "Optical properties of aerosols of mixed composition," Atmos. Environ. **18**(4), 871–878 (1984).
12. G. Gouesbet, B. Maheu, and G. Gréhan, "Light scattering from a sphere arbitrarily located in a Gaussian beam, using a Bromwich formulation," J. Opt. Soc. Am. A **5**(9), 1427–1443 (1988).
13. K. F. Ren, G. Gréhan, and G. Gouesbet, "Laser sheet scattering by spherical particles," Part. Part. Syst. Charact. **10**(3), 146–151 (1993).
14. K. F. Ren, G. Gréhan, and G. Gouesbet, "Evaluation of laser-sheet beam shape coefficients in generalized Lorenz-Mie theory by use of a localized approximation," J. Opt. Soc. Am. A **11**(7), 2072–2079 (1994).
15. F. Onofri, G. Gréhan, and G. Gouesbet, "Electromagnetic scattering from a multilayered sphere located in an arbitrary beam," Appl. Opt. **34**(30), 7113–7124 (1995).
16. F. Onofri, D. Blondel, G. Gréhan, and G. Gouesbet, "On the optical diagnosis and sizing of spherical coated and multilayered particles with phase-Doppler anemometry," Part. Part. Syst. Charact. **13**(2), 104–111 (1996).
17. P. Yang and K. N. Liou, "Finite-difference time domain method for light scattering by small ice crystals in three-dimensional space," J. Opt. Soc. Am. A **13**(10), 2072–2085 (1996).
18. M. I. Mishchenko, J. W. Hovenier, and L. D. Travis, "Light scattering by nonspherical particles," J. Quant. Spectrosc. Radiat. Transfer **63**(2-6), 127–129 (1999).
19. L. Bi, P. Yang, G. W. Kattawar, Y. X. Hu, and B. A. Baum, "Scattering and absorption of light by ice particles: Solution by a new physical-geometric optics hybrid method," J. Quant. Spectrosc. Radiat. Transfer **112**(9), 1492–1508 (2011).
20. D. W. Mackowski and M. I. Mishchenko, "Direct simulation of multiple scattering by discrete random media illuminated by Gaussian beams," Phys. Rev. A **83**(1), 013804 (2011).
21. Y. Han, Z. Cui, and W. Zhao, "Scattering of Gaussian beam by arbitrarily shaped particles with multiple internal inclusions," Opt. Express **20**(2), 718–731 (2012).
22. Q. Shang, Z. Wu, T. Qu, Z. Li, L. Bai, and L. Gong, "Analysis of the radiation force and torque exerted on a chiral sphere by a Gaussian beam," Opt. Express **21**(7), 8677–8688 (2013).
23. A. M. Yao and M. J. Padgett, "Orbital angular momentum: Origins, behavior and applications," Adv. Opt. Photonics **3**(2), 161–204 (2011).
24. A. E. Willner, H. Huang, Y. Yan, Y. Ren, N. Ahmed, G. Xie, C. Bao, L. Li, Y. Cao, Z. Zhao, J. Wang, P. J. Martin, M. Tur, S. Ramachandran, A. F. Molisch, N. Ashrafi, and S. Ashrafi, "Optical communications using orbital angular momentum beams," Adv. Opt. Photonics **7**(1), 66–106 (2015).
25. N. Bozinovic, Y. Yue, Y. Ren, M. Tur, P. Kristensen, H. Huang, A. E. Willner, and S. Ramachandran, "Terabit-Scale Orbital Angular Momentum Mode Division Multiplexing in Fibers," Science **340**(6140), 1545–1548 (2013).
26. M. P. J. Lavery, F.C. Speirits, S. M. Barnett, and M. J. Padgett, "Detection of a Spinning Object Using Light's Orbital Angular Momentum," Science **341**(6145), 537–540 (2013).
27. F. G. Mitri, "Electromagnetic wave scattering of a high-order Bessel vortex beam by a dielectric sphere," IEEE Trans. Antennas Propag. **59**(11), 4375–4379 (2011).
28. T. Qu, Z. Wu, Q. Shang, Z. Li, J. Wu, and H. Li, "Scattering and propagation of a Laguerre-Gaussian vortex beam by uniaxial anisotropic bispheres," J. Quant. Spectrosc. Radiat. Transfer **209**, 1–9 (2018).

Optics EXPRESS

29. W. B. Wang, R. Gozali, L. Shi, L. Lukas, and R. R. Alfano, "Deep transmission of Laguerre-Gaussian vortex beams through turbid scattering media," Opt. Lett. **41**(9), 2069–2072 (2016).
30. M. Yang, Y. Wu, K. F. Ren, and X. Sheng, "Computation of radiation pressure force exerted on arbitrary shaped homogeneous particles by high-order Bessel vortex beams using MLFMA," Opt. Express **24**(24), 27979–27992 (2016).
31. A. Chen, J. Wang, Y. Han, Z. Cui, and M. Yu, "Implementation of nondiffracting Bessel beam sources in FDTD for scattering by complex particles," Opt. Express **26**(20), 26766–26775 (2018).
32. Q. Huang, M. Cheng, L. Guo, J. Li, X. Yan, and S. Liu, "Scattering of aerosol particles by a Hermite-Gaussian beam in marine atmosphere," Appl. Opt. **56**(19), 5329–5335 (2017).
33. L. Cicchitelli, H. Hora, and R. Postle, "Longitudinal field components for laser beams in vacuum," Phys. Rev. A **41**(7), 3727–3732 (1990).
34. K. F. Ren, G. Gouesbet, and G. Gréhan, "Integral localized approximation in generalized Lorenz-Mie theory," Appl. Opt. **37**(19), 4218–4225 (1998).
35. J. A. Lock, "Interpretation of extinction in Gaussian-beam scattering," J. Opt. Soc. Am. A **12**(5), 929–938 (1995).
36. G. Hanel, "The properties of atmospheric aerosol particles as functions of the relative humidity at thermodynamic equilibrium with the surrounding moist air," Adv. Geophys. **19**(C), 73–188 (1976).
37. G. Hanel, "The real part of the mean complex refractive index and the mean density of samples of atmospheric aerosol particles," Tellus **20**(3), 371–379 (1968).
38. H. Du, L. Kong, T. Cheng, J. Chen, J. Du, L. Li, X. Xia, C. Leng, and G. Huang, "Insights into summertime haze pollution events over Shanghai based on online water-soluble ionic composition of aerosols," Atmos. Environ. **45**(29), 5131–5137 (2011).